Designing real-time biosensors and chemical sensors based on symmetrical photonic crystal heterostructures

M. Sharifi [a], P. Tajalli [b], H. Pashaei Adl [c], H. Tajalli [d,*]

[a] Faculty of Physics, University of Tabriz, Tabriz, Iran.
[b] Institut für Theoretische Physik, Universität Regensburg, 930400, Regensburg, Germany.
[c] Instituto de Ciencia de Materiales (ICMUV), Universidad de Valencia, C/ Catedrático José Beltrán 2, 46980 Paterna, Spain.
[d] Biophotonic Research Center, Tabriz Branch Islamic Azad University, Tabriz, Iran

*** Corresponding author email: tajallihabib@gmail.com**

Received: Nov. 3, 2021, Revised: Dec. 21, 2021, Accepted: Feb. 26, 2022, Available Online: Mar. 8, 2022
DOI: 10.30495/ijbbo.2021.689422

ABSTRACT— In this paper, we introduce and analytically demonstrate a novel biosensor based on the light-matter interaction in a classic topological photonic crystal (PC) heterostructure, which consists of two opposite-facing 5-period PCs separated by a microfluidic channel. Because of the excitation of topological edge mode (TEM) at the interface of the two PCs, the strong coupling between incident light and TEM produces a high-quality resonance peak, that can be used to detect very small changes in the refractive index of biomaterials such as Jurkat Cells inside the microfluidic channel. The proposed biosensor has a sensitivity as high as 240 nm/RIU and figure of merit (FOM) higher than 250.

Keywords: Biosensor, Photonic Crystals, Topological Edge Modes, Light-Matter interaction, Transfer Matrix Method.

I. INTRODUCTION

Sensors are the results of a fast-growing discipline in the areas of biological, chemical, and physical sciences with a wide range of applications in engineering and computer. For example, electrochemical biosensors [1,2], thermal biosensors [3], resonant biosensors [3], optical biosensors [4-6], refractometry biosensing [7-10] and so on, are various types of biosensors with diverse operational range . Sensors have been used in medicine and life sciences for monitoring patients, and diagnosing deseas, in order to improve the health care [11]. Many innovative sensors have been developed in response to the demand for the early disease detection and diagnosis, as well as in the minimally invasive detection technologies [12]. Clinical diagnosis relies heavily on the sensitive detection of biomolecules or chemicals, especially in the case of illnesses, where early discovery might improve recovery and survival chances. Optical biosensors have gained increasing attention for their capacity to identify early diseases such as Alzheimer's [13], cancer [14], and biomolecular assay measures due to their simplicity and high sensitivity. In this type of biosensors, the information is gathered by the measurement of photons (rather than electrons as in the case of electrodes). It is ideal to utilize optical biosensors to identify cancer since cancer cells have a higher refractive index than healthy cells due to the increased amount of protein in their nuclei.

Additionally, from both theoretical and practical viewpoints, manipulating light-matter interactions in the weakly and strongly coupled nanostructures, have gained too much attention [15–17]. Optical microcavities [18–19], plasmonic nanostructures [20–22], multilayered structures [23–27], and metallic nanostructures [28–30] are examples of hybrid systems with strong coupling. Because of their unique energy transfer and larger modulation properties , it is ideal for studying light-matter

interactions. Photonic topological insulators have recently received a lot of attention in the integrated optics due to their unique properties of topologically protected edge states [31]. Many schemes for constructing topological photonic modes have been proposed. The one-dimensional (1D) topological PC structure [32-34] is favored among all of those structures because of its advantages in having a simple design and fabrication properties. These findings suggest that a 1D PC heterostructure with robust topological features can be developed to excite topological edge mode, thus, consequently increasing light-matter interaction.

In, this paper, we have developed a novel optical biosensor by manipulating the strong light-matter interaction in a 1D topological PC heterostructure with a microfluidic channel in between. With proper design, TEM excited at the interface between the two opposite-facing PCs, so a perfect transmission peak is observed when the incident light is perfectly coupled to the TEM. We demonstrated that the perfect transmission can be tuned by varying the thickness of the microfluidic channel in order to detect changes in the refractive index of the biomaterials inside the channel. The TEM-induced high-quality resonance is used to design a supersensitive biosensor with sensitivity as high as, S=240 nm/RIU, and figure of merit higher than 250. It is worthy to note that, we tested our optical biosensor with the Jurkat cells [4]. This biological cell is a reference cell for diagnosing leukemia [35]. Leukemia is a progressive and malignant disease of the body's hematopoietic organs, and can affect the brain, blood cells, Affect the lymph nodes, and other parts of the lymphatic system. If diagnosed early, it can cure up to 90% of cases.

II. STRUCTURE AND BASIC EQUATIONS

The proposed structure, $(AB)^N F(BA)^N$, consists of a microfluidic channel F, sandwiched between two opposite-facing 5-period PCs, to sense small changes in the refractive index of the fluid (see figure 1(a)). A, B consists of Si and SiO_2 layers, respectively, with refractive indices being n_A= 2.82 and n_B = 1.46 [36]. The thickness of the unit cell is $\Lambda = \lambda_c/4n_A + \lambda_c/4n_B$, where the central wavelength is λ_c= 700 nm. The thicknesses of Si and SiO_2 are set to d_A = 0.4 Λ and d_B = 0.6 Λn respectively. For ease of the calculations, the TE polarized light with normal incidence to the surface is considered. The electric field equations in layers can be written as:

$$\vec{E}_j(x,y) = E(z)e^{i(k_x x k_{zj} z)\hat{e}_y} \tag{1}$$

Where $k_x = k_0 \sin\theta$, $k_0 = \omega / c$, $k_{zj} = k_0\sqrt{\varepsilon_j \mu_j (1-\sin\theta^2/\varepsilon_j\mu_j)}$, and θ being the angle of the of the incident light beam. Inside the layers, the electric field is governed by the Helmholtz equation [37]:

$$\frac{d^2E}{dz^2} + \left(\varepsilon_j \mu_j \omega^2 / c^2\right)E = 0 \tag{2}$$

with subscript j denoting the number of the layers. At the interface between two layers, we can apply the boundary conditions [38]:

$$\begin{aligned} E_+ &= E_- \\ \frac{1}{\mu_+}\frac{dE}{dz_+} &= \frac{1}{\mu_-}\frac{dE}{dz_-} \end{aligned} \tag{3}$$

Therefore, by applying the boundary conditions in the interfaces between layers, we can employ the transfer matrix to combine the electric field at z and z + Δz [39, 40]:

$$m_l(\Delta z_j) = \begin{pmatrix} \cos(k_{zj}\Delta z_j) & -\frac{\mu_j\omega}{k_{zj}c}\sin(k_{zj}\Delta z_j) \\ \frac{k_{zj}c}{\mu_j\omega}\sin(k_{zj}\Delta z_j) & \cos(k_{zj}\Delta z_j) \end{pmatrix} \tag{4}$$

Here, $l = 1, 2, \ldots, N$, where N is the total number of the layers in the structure. So, the global transfer matrix can be written as, $M^g = \prod_{l=1}^{N} m_l(\Delta z_j)$. The tangential components of the electric and magnetic fields at incident site $z = 0$ and the transmitted site $z = L$ are related by the following matrix equation:

$$\begin{pmatrix} E_{y1} \\ H_{x1} \end{pmatrix}_{z=0} = M^{g} \begin{pmatrix} E_{yN} \\ H_{xN} \end{pmatrix}_{z=L} \quad (5)$$

Finally, the transmission can be obtained as $T = tt^{*}$, where $t = 2p/(pM_{11}^{g} + M_{22}^{g} + M_{12}^{g} + M_{21}^{g})$ and $p = \cos\theta$. The subscript "j" in equation 4 represents the linear layer (A, B, F), with the thicknesses of d_A, d_B and d_F.

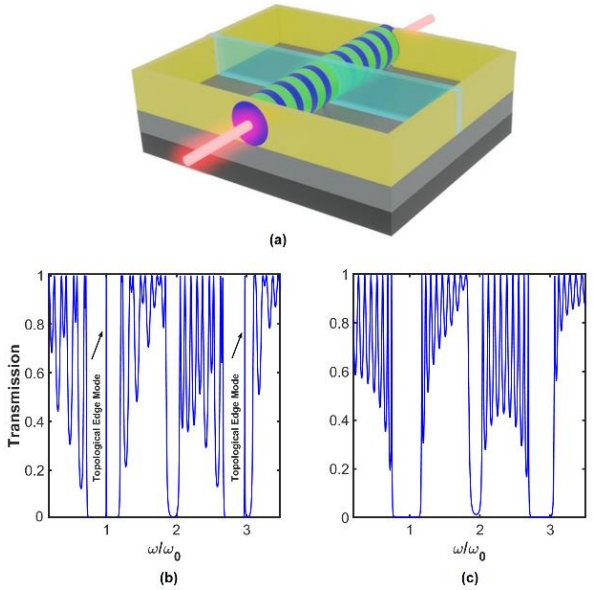

Fig. **1** (a) Schematic of the proposed biosensor. The blue and green layers are A and B layers, and transparent faded blue in the center is a microfluidic channel, F. (b), (c) The transmission spectra of symmetry $((AB)^5(BA)^5)$ with d_F=0, and typical PC $((AB)^{10})$.

III. RESULTS AND DISCUSSION

According to the Figure 1, the band gap position of the symmetry PC is the same as that of the typical PC. However, due to the inverse arrangement of a unit cell, the two PCs have different topological properties. Thus, the TEM can be excited in these two gaps simultaneously by constructing an interface with PC on one side and symmetry PC on the other side. In other words, simple photonic crystals have these well-known photonic band gaps in specific frequency ranges (Fig. 1 (c)), and by engineering the geometry (merely changing the order of the layers), the distinct TEM can be excited through the specific band gaps (Fig. 1 (b)). According to previous research [33, 41, 42], the TEM can be excited at the interface of a 1D PC heterostructure when the two PCs have different topological properties [41, 42] in the overlapping gap. Another important feature of these symmetric structures is that their photonic band gaps do not move, and their band gaps correspond exactly with simple photonic crystals but with TEM through some of them (Fig. 1 (b)). Figure 1(b) clearly shows the TEM in the transmission spectrum of the proposed structure without a microfluidic channel (d_F=0). When an incident light irradiates the suggested multilayer structure, TEM can be excited at the interface of a topological PC heterostructure. The incident light and TEM can be strongly coupled, resulting in a sharp peak in the reflection (or transmission) spectrum. Furthermore, the resonant point can be manipulated by changing the thickness of the defect layer. The refractive index of the fluid inside the channel is set to n_F = 1.35, which is the refractive index of healthy Jurkat Cells [4].

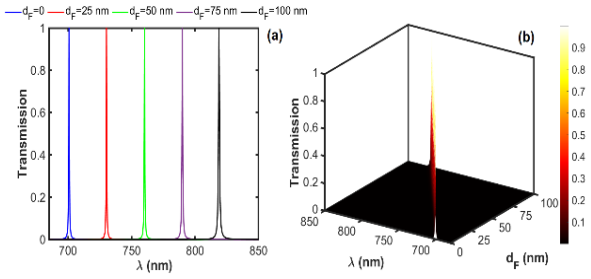

Fig. **2** (a) Transmission spectra of the system as a function of wavelength with different microfluidic channel widths (b) 3D representation of Transmission spectra as a function of wavelength while the thickness of the microfluidic channel continuously changing from 0-100 nm.

Figures 2(a) and 2(b) show how transmission varies with incident wavelength under different microfluidic channel thicknesses. High-quality resonance is observed, and the resonant wavelength can be tuned continuously with a small change in the thickness of the fluidic channel, d_F. The transmission peak produced by the strong coupling of incident light and TEM approaches 100%, and the full width at half-maximum (FWHM) of the resonant peak is less than 1 nm. The normalized electric field intensity distributions at 700.6 nm and 818.8 nm when d = 0 and 100 nm are shown in Figs. 3(a) and 3(b) to better illustrate the TEMs excited in the multilayer system. It is revealed

that the majority of the electric field's energy is concentrated near the interface between the two opposite-facing PCs, allowing for strong light-matter interaction. The fine-tuning of the structure (changing the thickness of the microfluidic channel) does not affect the transmission performance, and the electric field distribution is the same as before. These results show that the topological properties of the structures and their associated edge states are very robust to structural disturbances.

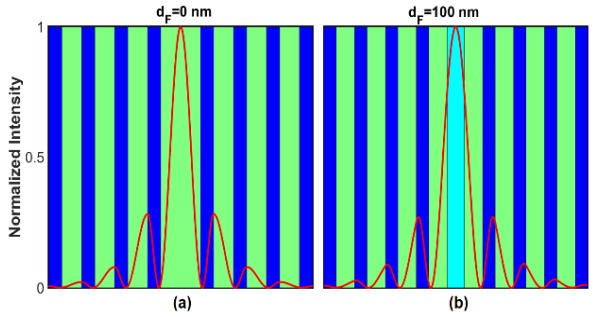

Fig. **3** Normalized electric field profile distributions at 700.6 nm and 818.8 nm when d_F = 0 and 100 nm.

As previously stated, when TEM is excited, the majority of the field energy is concentrated in the microfluidic channel, and any change in the channel (e.g., thickness and refractive index) affects the resonant wavelength. As a result, the proposed optical biosensor will have extremely high sensitivity due to its ultra-narrow transmission line bandwidth. The sensing capability was evaluated by computing the shift in the resonant wavelength per unit change in the refractive index, $S = \Delta\lambda/\Delta n_F$.

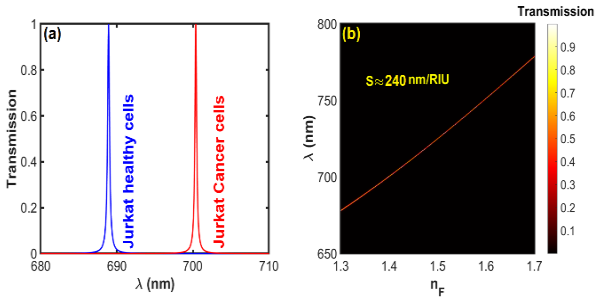

Fig. **4** Transmission spectra of the system (a) as a function of wavelength for healthy (n_F=1.345) and cancer (n_F=1.395) Jurkat cells, (b) when n_F continuously changes from 1.3 to 1.7, in this figure sensitivity of sensor evaluated as high as 240 nm/RIU, while d_F = 500 nm.

Figure 4(a) depicts the system's transmission spectra (d_F = 500 nm) for two different values of the biomaterials refractive index, which corresponds to healthy (n_F=1.345) and cancer (n_F=1.395) Jurkat cells [4]. We can see that the resonant wavelength is positively correlated with n_F and increases linearly with n_F. (See figure 4b). The slope of the fitted curve indicates that the sensitivity S is 240 nm/RIU.

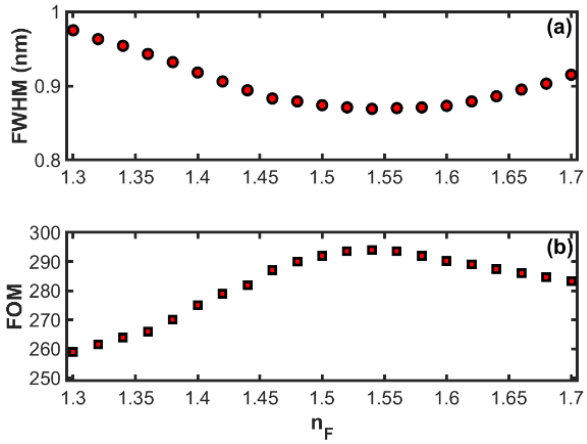

Fig. **5** Calculated (a) FWHM, and (b) FOM values of the resonant mode as a function of the refractive index of the microfluidic channel.

To calculate the FOM of the proposed structure, which can be defined as the sensitivity to FWHM ratio, FOM = S/FWHM, the FWHM of the resonance peak shown in Fig. 5(a) is used. The FOM surpassed 250 (see Fig. 5(b)), which can be attributed to the ultranarrow linewidth of the resonance peaks (less than 1 nm), as shown in Fig. 5(b). It should be noted that,because of the numerous advantages of the proposed heterostructure, including the robustness of the topological properties of the structures and their associated edge states, very high light-matter interaction between the two opposite-facing PCs as a result of the electric field's energy concentration near this interface, and very narrow TEM with high Q-factor, this device's sensing capability exceeds many sensors reported in the literature [43–45].

IV. CONCLUSION

In this study, we introduce and analyze a novel biosensor based on light-matter interaction in a classic topological photonic crystal (PC) heterostructure. Because of the strong coupling

of light and TEM at the interface of the two PCs, a high-quality resonance peak (high transmission, narrow bandwidth) occurs in the configuration, and this excellent transmission response was used to design a super highly sensitive biosensor with a sensitivity of 240 nm/RIU and FOM higher than 250.

REFERENCES

[1] D. Grieshaber, R. MacKenzie, J. Vörös, E. Reimhult, "Electrochemical biosensors-sensor principles and architectures," Sensors, Vol. 8, pp. 1400-1458, 2008.

[2] O. A. Sadik, A.O. Aluoch, and A. Zhou, "Status of biomolecular recognition using electrochemical techniques," Biosensors Bioelectron. Vol. 24, pp. 2749–2765, 2009.

[3] R. S. Marks, D. Cullen, C. Lowe, H. H. Weetall, and I. Karube, *Handbook of Biosensors and Biochips. Hoboken*, NJ, USA: Wiley, 2007.

[4] M. Sharifi, H. Pashaei Adl, H. Tajalli, and A. Bahrampour, "Design of a Surface Plasmon resonance biosensor with one dimensional photonic crystals to diagnosis of cancer," Iranian Journal of Physics Research, Vol. 16, pp. 133-138, 2016.

[5] F. Baldini, A. N. Chester, J. Homola, and S. Martellucci, *Optical Chemical Sensors*, The Netherlands: Springer, 2006.

[6] F. Bayat, S. Ahmadi-Kandjani, and H. Tajalli "Designing real-time biosensors and chemical sensors based on defective 1-D photonic crystals," IEEE Photon. Technol. Lett. Vol. 28, pp. 1843–1846, 2016.

[7] S. Mariani, L. Pino, L. M. Strambini, L. Tedeschi, and G. Barillaro, "10000-fold improvement in protein detection using nanostructured porous silicon interferometric aptasensors," ACS Sensors, Vol. 1, pp. 1471–1479, 2016.

[8] S. Mariani, L. Pino, L.M. Strambini, L. Tedeschi, and G. Barillaro, "Femtomole detection of proteins using a label-free nanostructured porous silicon interferometer for perspective ultrasensitive biosensing," ACS Anal. Chem. Vol. 17, pp. 8502–8509, 2016.

[9] S. Surdo, F. Carpignano, L.M. Strambini, S. Merlo, and G. Barillaro, "Capillarity-driven (self-powered) one-dimensional photonic crystals for refractometry and (bio) sensing applications," RSC Adv. Vol. 4, pp. 51935–51941, 2014.

[10] H. Pashaei Adl, F. Bayat, N. Ghorani, S. Ahmadi-Kandjani, H. Tajalli, "A defective 1-D photonic crystal-based chemical sensor in total internal reflection geometry," IEEE Sensors, Vol. 17, pp. 4046-4051, 2017.

[11] Patolsky F, G. Zheng, and C.M. Lieber, "Nanowire sensors for medicine and the life sciences," Nanomedecine. Vol. 1, pp. 51-65, 2006.

[12] N.M.M. Pires, T. Dong, U. Hanke, and N. Hoivik, "Recent developments in optical detection technologies in lab-on-a-chip devices for biosensing applications," Sensors. Vol. 14, pp. 15458-15479, 2014.

[13] A. J. Haes, L. Chang, W.L. Klein, and R. P. Van Duyne "Detection of a biomarker for Alzheimer's disease from synthetic and clinical samples using a nanoscale optical biosensor," J. Amer. Chem. Soc. Vol. 127, pp. 2264–2271, 2005.

[14] H. S. Jang, K. No Park, Ch. Duk Kang, J. Pyo Kim, S. Jun Sim, and K. Shik Lee, "Optical fiber SPR biosensor with sandwich assay for the detection of prostate specific antigen," Opt. Commun. Vol. 282, pp. 2827–2830, 2009.

[15] S. Balci and C. Kocabas, "Ultra hybrid plasmonics: strong coupling of plexcitons with plasmon polaritons," Opt. Lett. Vol. 40, pp. 3424–3427, 2015.

[16] W. Wang, P. Vasa, R. Pomraenke, R. Vogelgesang, A. De Sio, E. Sommer, M. Maiuri, C. Manzoni, G. Cerullo, and Ch. Lienau, "Interplay between Strong Coupling and Radiative Damping of Excitons and Surface Plasmon Polaritons in Hybrid Nanostructures," ACS Nano, Vol. 8, pp. 1056–1064, 2014.

[17] L. Shi, T.K. Hakala, H.T. Rekola, J.P. Martikainen, R. J. Moerland, and P. Törmä, "Spatial Coherence Properties of Organic Molecules Coupled to Plasmonic Surface Lattice Resonances in the Weak and Strong Coupling Regimes," Phys. Rev. Lett. Vol. 112, pp. 153002 (1-22), 2014.

[18] F. Barachati, J. Simon, Y. A. Getmanenko, S. Barlow, S. R. Marder, and S. Kéna-Cohen, "Tunable Third-Harmonic Generation from Polaritons in theUltrastrong Coupling

Regime," ACS Photonics, Vol. 51, pp. 119–125, 2018.

[19] R.-Q. Li, D. Hernángomez-Pérez, F. J. García-Vidal, and A. I. Fernández-Domínguez, "Transformation Optics Approach to Plasmon-Exciton Strong Coupling in Nanocavities," Phys. Rev. Lett. Vol. 117, pp. 10740 (1-12), 2016.

[20] Y. M. Qing, H.F. Ma, and T.J. Cui "Investigation of strong multimode interaction in a graphene-based hybrid coupled plasmonic system," Carbon, Vol. 145, pp. 596–602, 2019.

[21] Y. M. Qing, H.F. Ma, and T.J. Cui "Theoretical Analysis of Tunable Multimode Coupling in a Grating-Assisted Double-Layer Graphene Plasmonic System," ACS Photonics, Vol. 6, pp. 2884–2893, 2019.

[22] J. Nong, W. Wei, W. Wang, G. Lan, Zh. Shang, J. Yi, and L. Tang "Strong coherent coupling between graphene surface plasmons and anisotropic black phosphorus localized surface plasmons," Opt. Express, Vol. 26, pp. 1633–1644, 2018.

[23] Y. M. Qing, H.F. Ma, and T.J. Cui, "Flexible control of light trapping and localization in a hybrid Tamm plasmonic system," Opt. Lett. Vol. 44, pp. 3302–3305, 2019.

[24] J. Hu, W. Liu, W. Xie, W. Zhang, E. Yao, Y. Zhang, and Q. Zhan "Strong coupling of optical interface modes in a 1D topological photonic crystal heterostructure/Ag hybrid system," Opt. Lett. Vol. 44, pp. 5642–5645, 2019.

[25] H. Lu, Y. Li, H. Jiao, Z. Li, D. Mao, and J. Zhao, "Induced reflection in Tamm plasmon systems," Opt. Express, Vol. 27, pp.5383–5392, 2019.

[26] J. P. Martinez-Pastor, H. Pashaei Adl, S. Gorji, J. Navarro-Arenas, G. Muñoz-Matutano, I. Suárez, V. S. Chirvony, A. F. Gualdrón-Reyes, and I. Mora-Seró "Lead halide perovskite nanocrystals: optical properties and nanophotonics", In Low-Dimensional Materials and Devices, Vol. 11800, pp. 1180013, 2021

[27] H. Pashaei Adl, S. Gorji, M. Karimi Habil, I. Suárez, V. S. Chirvony, A. F. Gualdrón-Reyes, I. Mora-Seró, L. M. Valencia, M. de la Mata, J. Hernández-Saz, S. I. Molina, C. J. Zapata-Rodríguez, and J. P. Martínez-Pastor, "Purcell enhancement and wavelength shift of emitted light by CsPbI3 perovskite nanocrystals coupled to hyperbolic metamaterials," ACS photonics, Vol. 7, pp. 3152-3160, 2020.

[28] G. Zengin, M. Wersäll, S. Nilsson, T. J. Antosiewicz, M. Käll, and T. Shegai, "Realizing Strong Light-Matter Interactions between Single-Nanoparticle Plasmons and Molecular Excitons at Ambient Conditions," Phys. Rev. Lett. Vol. 114, pp. 157401, 2015.

[29] Q. Y. Lin, Zh. Li, K. A. Brown, M. N. O'Brien, M. B. Ross, Y. Zhou, S. Butun, P.-Ch. Chen, G. C. Schatz, V. P. Dravid, K. Aydin, and Ch. A. Mirkin, "Strong Coupling between Plasmonic Gap Modes and Photonic Lattice Modes in DNA-Assembled Gold Nanocube Arrays," Nano Lett. Vol. 15, pp. 4699–4703, 2015.

[30] A. Benz, S. Campione, J. F. Klem, M. B. Sinclair, and I. Brener, "Control of Strong Light-Matter Coupling Using the Capacitance of Metamaterial Nanocavities," Nano Lett. Vol. 15, 1959–1966, 2015.

[31] L. Lu, J. D. Joannopoulos, and M. Soljacic, "Topological photonics," Nat. Photonics, Vol. 8, pp. 821–829, 2014.

[32] X. Wang, Y. Liang, L. Wu, J. Guo, X. Dai, and Y. Xiang, "Multi-channel perfect absorber based on a one-dimensional topological photonic crystal heterostructure with graphene," Opt. Lett. Vol. 43, pp. 4256–4259, 2018.

[33] W. Gao, X. Hu, Ch. Li, J. Yang, Zh. Chai, J. Xie, and Q. Gong, "Fano-resonance in one-dimensional topological photonic crystal heterostructure," Opt. Express, Vol. 26, pp. 8634–8644, 2018.

[34] L. Wang, X. Hu, Ch. Li, J. Yang, Zh. Chai, J. Xie, and Q. Gong, "Zak phase and topological plasmonic Tamm states in one-dimensional plasmonic crystals," Opt. Express, Vol. 26, pp. 28963–28975, 2018.

[35] M. S. Jazi, S. Mohammadi, Yaghoub Yazdani, S. Sedighi, A. Memarian, and Mehrdad Aghaei,"Effects of valproic acid and pioglitazone on cell cycle progression and proliferation of T-cell acute lymphoblastic leukemia Jurkat cells. Iranian journal of basic medical sciences," Vol. 19, pp. 779-789, 2014.

[36] X. Wang, Y. Liang, L. Wu, J. Guo, X. Dai, Y. Xiang, "Multi-channel perfect absorber based on a one-dimensional topological photonic crystal heterostructure with grapheme," Optics letters, Vol. 43, pp.4256-4259, 2018.

[37] S. M. Wang and L. Gao, “Nonlinear responses of the periodic structure composed of single negative materials,” Opt. Commun., Vol. 281, pp. 197–204, 2006.

[38] H. Pashaeiadl, M. Naserpour, and C. J. Zapata-Rodriguez,"Scattering of electromagnetic waves by a graphene-coated thin cylinder of left-handed metamaterial," Optik, Vol. 159, pp. 123-132, 2018.

[39] S. R. Entezar, et al. “Optical isolation via one-dimensional magneto-photonic crystals containing nonlinear defect layer,” Opt. Commun., Vol. 352, pp. 91–95, 2015.

[40] B. T. Moghaddam, S. R. Entezar, and H. Pashaei Adl, "Nonlinear properties of a graded-index photonic heterostructure," Pramana, Vol. 80, pp. 887-894, 2013.

[41] Y. M. Qing, H. F. Ma, L. Wei Wu, and T. Jun Cui “Manipulating the light-matter interaction in a topological photonic crystal heterostructure,” Opt. Express. Vol. 28, pp. 34904-34915, 2020.

[42] D. Gao, W. Mao, R. Zhang, J. Liu, Q. Zhao, and W.Y. Tam, “Tunable interface state in one dimensional composite photonic structure” Opt. Comm. Vol. 453, pp. 124324, 2019.

[43] R. Ameling, Lutz Langguth, M. Hentschel, M. Mesch, P. V. Braun, and H. Giessen, “Cavity-enhanced localized plasmon resonance sensing,” Appl. Phys. Lett. Vol. 97, pp. 253116 (1-3), 2010.

[44] J. Ye and P. Van Dorpe, “Improvement of Figure of Merit for Gold Nanobar Array Plasmonic Sensors,” Plasmonics, Vol. 6, pp. 665–671, 2011.

[45] C. Huang, Ch. Huang, J. Ye, Sh. Wang, T. Stakenborg, and L. Lagae, “Gold nanoring as a sensitive plasmonic biosensor for on-chip DNA detection,” Appl. Phys. Lett. Vol. 100, pp. 173114, 2012.

THIS PAGE IS INTENTIONALLY LEFT BLANK.